

Dynamic stall due to unsteady marginal separation

By J. W. ELLIOTT

Department of Applied Mathematics, University of Hull, Hull HU6 7RX, UK

AND F. T. SMITH

Department of Mathematics, University College London, London WC1E 6BT, UK

(Received 20 May 1986)

A theoretical investigation into the next stage of dynamic stall, concerning the beginnings of eddy shedding from the boundary layer near an aerofoil's leading edge, is described by means of the unsteady viscous–inviscid interacting marginal separation of the boundary layer. The fully nonlinear stage studied in the present paper is shown to match with a previous ‘weakly nonlinear’ regime occurring in the earlier development of the typical eddy from its initially slender thin state. Numerical solutions followed by linear and nonlinear analysis suggest that with confined initial conditions the strong instabilities in the present unsteady flow tend to force a breakdown within a finite time. This leads on subsequently to an unsteady predominantly inviscid stage where the eddy becomes non-slender, spans the entire boundary layer and its evolution then is governed by the Euler equations. This is likely to be followed by the shedding of the eddy from the boundary layer.

1. Introduction

Dynamic stall is associated with, and has its beginnings in, the breakdown of streamlined flow past an inclined aerofoil and this occurs often in practice: see below. The continued theoretical study of such a breakdown seems desirable and here we attempt to investigate the breakdown in terms of unsteady marginal interactive separation at high Reynolds numbers. In such separations the overall flow field initially displays only small local flow reversals which are embedded in the thin attached boundary layer on the aerofoil surface, but it is believed that these can subsequently erupt through and out of the boundary layer. The theoretical approach in this paper has applications to several areas of research, where the breakdown of streamlined flow also occurs, although the main context of the present study is external aerodynamics. We restrict ourselves here to essentially planar flow past a streamlined aerofoil.

The usual setting for dynamic stall is on slowly oscillating aerofoils, turbine blades or helicopter blades. The slow raising of the angle of attack may cause, initially, a separation and a recirculatory eddy flow only near the trailing edge of the aerofoil. This seems to be a relatively passive event, however, with the aerofoil motion remaining predominantly streamlined as the point of separation moves gradually upstream with increasing angle of attack. It is in sharp contrast to the sudden appearance, close to the leading edge, of a further eddy later in the cycle of oscillation, at higher angles of attack. This latter eddy, or sometimes more than one, amplifies and is ejected from the surface of the aerofoil, leading to the disruption of the entire flow field downstream. The main experimental and theoretical features of such a

dynamic stall are described by McAllister & Carr (1979), McCroskey (1982), Smith (1982) and Smith & Elliott (1985). The origins of the process have been viewed theoretically by Smith (1982) and Ryzhov & Smith (1984) in terms of marginal separation, and their predictions seem to be qualitatively in line with the main experimental observations. The theory is summarized below.

We consider the two-dimensional unsteady laminar flow of an incompressible fluid, of density ρ_∞ and kinematic viscosity ν_∞ , past a smooth aerofoil of thickness h_∞ , chord length l_∞ and with a rounded leading edge. The Reynolds number $Re = U_\infty l_\infty / \nu_\infty$ is assumed to be large. Here U_∞ is the speed of the oncoming mainstream, which is inclined at a small angle of attack α to the aerofoil. Cartesian coordinates $l_\infty x^*$, $l_\infty y^*$ fixed in the aerofoil, with corresponding velocity components $U_\infty u^*$, $U_\infty v^*$, are taken such that $(x^*, y^*) = (0, 0)$, $(1, 0)$ are the leading and trailing edges respectively. If p_∞ is the free-stream pressure then we write the pressure as $p_\infty + \rho_\infty U_\infty^2 p$ and the time as $l_\infty t^* / U_\infty$. For $Re \gg 1$, then, provided that the thickness-to-chord ratio is sufficiently small, say $h_\infty / l_\infty = O(\alpha)$, the flow past the aerofoil remains fairly streamlined. That is, over most of the flow field the flow is only a slight deviation from the uniform stream $u^* = 1$, $v^* = 0$, while the boundary layer remains attached to the aerofoil surface even in the neighbourhood of the trailing edge if the trailing edge is sharp enough, and the typical timescale t^* is $O(1)$.

The crucial area of interest now is the nonlinear zone of extent $O(\alpha^2)$ in x^* and y^* at the leading edge, where effectively the Navier–Stokes equations reduce to the inviscid potential-flow equations for flow past a semi-infinite parabola at a finite scaled angle of attack σ , subject to the condition of tangential flow along the aerofoil. Hence an unsteady inviscid tangential slip velocity $U_e(x, t)$ is set up along the parabola surface $n = 0+$, and we shall assume U_e is known. Here $\alpha^2 x$ is the normalized distance along the surface from the front stagnation point, $\alpha^2 n$ denotes the distance normal to the surface and t is the small timescale given by $t^* = \alpha^2 t$. The velocity is reduced to rest by means of a thin viscous boundary layer, governed by the classical equations

$$u = \frac{\partial \psi}{\partial y}, \quad v = \frac{-1}{(\alpha^2 Re)^{1/2}} \frac{\partial \psi}{\partial x}, \quad (1.1a)$$

$$\frac{\partial u}{\partial t} + u \frac{\partial u}{\partial x} - \frac{\partial \psi}{\partial x} \frac{\partial u}{\partial y} = \frac{\partial U_e}{\partial t} + U_e \frac{\partial U_e}{\partial x} + \frac{\partial^2 u}{\partial y^2}, \quad (1.1b)$$

where $y = (\alpha^2 Re)^{1/2} n$ is the boundary-layer coordinate and $\alpha^2 (\alpha^2 Re)^{-1/2} \psi$ is the stream function. Here u and v denote the tangential and normal velocity components respectively. These equations are subject to the conditions of no slip at the aerofoil surface,

$$u = \psi = 0 \quad \text{on } y = 0, \quad (1.1c)$$

and the requirement that the solution should match with the outer inviscid flow. Thus we require

$$\psi \sim U_e(x, t)[y - \delta(x, t)], \quad u \rightarrow U_e(x, t) \quad \text{as } y \rightarrow \infty, \quad (1.1d)$$

where $\delta^* = (\alpha^2 Re)^{-1/2} \delta(x, t)$ is the boundary-layer displacement which is to be found. Given a suitable starting form at $t = 0$, we are now in a position to integrate (1.1a–d) forward in time.

The leading-edge zone is, from above, of streamwise extent $O(\alpha^2)$ and of thickness $O(\alpha Re^{-1/2})$, where for self-consistency we see that α must be restricted to the range $Re^{-1/2} \ll \alpha \ll 1$. If α is reduced to $O(Re^{-1/2})$ the leading-edge zone becomes asymptotically indistinct from the $O(Re^{-1})$ region surrounding the leading edge which is governed

by the full Navier–Stokes equations. On the other hand for α of $O(1)$, there is in general virtually no attached flow over one of the aerofoil surfaces and the leading-edge region becomes asymptotically indistinct from the rest of the flow field with increasing α . The breakdown of the overall flow structure, when $Re^{-1/2} \ll \alpha \ll 1$, can take place first through the above unsteady boundary-layer flow in the nonlinear leading-edge zone. An alternative breakdown for unsteady boundary-layer flow is described by the work of Van Dommelen (1981) and Elliott, Cowley & Smith (1983), but that is more relevant to flows past bluff bodies, where no steady-state solution exists for a completely attached boundary layer, and a drastic, unsteady, breakdown at a finite time is inevitable. Our concern here is focused on marginal breakdown (Stewartson, Smith & Kaups 1982) where the solution to the steady-state version of (1.1*a–d*) exists or nearly exists. This seems a more appropriate context for aerodynamic stall.

In *steady* marginal flows the scaled skin friction $\tau = \partial u(x, 0)/\partial y$ becomes zero, or close to zero, in the neighbourhood of the regular separation point $x = x_c$. In fact τ acquires there either a parabolic form, with a positive minimum, or the form of the vanishing square-root singularity (Goldstein 1948), depending upon whether the scaled angle of attack σ defined above is less or greater than the critical value σ_c that corresponds to regular separation. Therefore the steady-state solution to (1.1*a–d*) ceases to exist about $x = x_c$ near $\sigma = \sigma_c$. A local order-of-magnitude analysis then indicates that, in a region of streamwise length $O(|\sigma - \sigma_c|^{1/2})$ about $x = x_c$, a thin viscous sublayer of thickness $O(|\sigma - \sigma_c|^{1/2})$ drives the flow, with a relatively slow local timescale $t = O(|\sigma - \sigma_c|^{-1/2})$ for *unsteady* marginal flow. This is in some sense a weakly nonlinear theory, with the local flow problem reducing to the study of an unsteady nonlinear integro–differential equation [(1.2) below]. As regards this equation, the case where $|\sigma - \sigma_c|$ is relatively large, greater than any inverse power of the effective Reynolds number $R_1 = \alpha^2 Re$, has been examined by Smith & Elliott (1985) for unsteady motion, while the case where $|\sigma - \sigma_c| = O(R_1^{-1/2})$ and interactive effects come into play has been studied by Stewartson *et al.* (1982) for steady motion and by Smith (1982) and Ryzhov & Smith (1984) for unsteady motion. For both of the unsteady regimes, classical and interactive, just mentioned, it was shown that the instabilities present in the local separated motion can accumulate to force a breakdown within a finite scaled time, for sufficiently confined initial disturbances. For example, Smith (1982) showed that if $x - x_c = R_1^{-1/2} \bar{x}$ and $t = R_1^{1/2} \bar{t}$ denote the short streamwise and slow temporal scales respectively, with the displacement of the form

$$\delta^* = R_1^{-1/2} \delta(x, t) = R_1^{-1/2} \{ \delta_0 + R_1^{-1/2} [\delta_1 \bar{x} + \bar{A}_s(\bar{x}, \bar{t})] + \dots \},$$

where δ_0, δ_1 are positive constants, then the displacement correction \bar{A}_s satisfies the equation (in normalized form)

$$\bar{A}_s^2 - \bar{x}^2 + 'O' = \int_{\bar{x}}^{\infty} \frac{\partial^2 \bar{A}_s}{\partial \xi^2} \frac{d\xi}{(\xi - \bar{x})^{1/2}} - \int_{-\infty}^{\bar{x}} \frac{\partial \bar{A}_s}{\partial \bar{t}} \frac{d\xi}{(\bar{x} - \xi)^{1/2}}, \tag{1.2}$$

where 'O' represents $O(1)$ -terms. The first integral here accounts for the interaction with the external mainstream and the second accounts for unsteady effects. With certain initial disturbances it was found that there is a singularity involving a nonlinear focusing about a position $\bar{x} = \bar{x}_s$ at a finite time $\bar{t} = \bar{t}_s$, with $\bar{A}_s \sim (\bar{t}_s - \bar{t})^{-1/2} \hat{A}_0(\hat{x})$ as $\bar{t} \rightarrow \bar{t}_s^-$. Here $\hat{x} = (\bar{x} - \bar{x}_s)/(\bar{t}_s - \bar{t})^{1/2}$ and \hat{A}_0 satisfies a nonlinear ordinary integro–differential equation [repeated in (2.5) below] which therefore fixes the terminal form for \bar{A}_s . The above focusing or breakdown implies that a new structure emerges when the time $(\bar{t}_s - \bar{t})$ is as small as $O(R_1^{-2/5})$, producing a shortened

lengthscale $|\bar{x} - \bar{x}_s|$ of $O(R_1^{-\frac{2}{3\delta}})$. In the new structure set up then, the new localized variables are X and T , where

$$x - x_c - R_1^{-\frac{1}{3}}\bar{x}_s = R_1^{-\frac{2}{3}}X, \quad t - R_1^{\frac{1}{3}}\bar{t}_s = R_1^{-\frac{1}{3}}T, \quad (1.3)$$

and at this stage ($X, T = O(1)$) a new, fully nonlinear, unsteady triple-deck interaction comes into play.

Our concern is with this next stage of the dynamic-stall phenomenon, governed by the scalings (1.3). In §2 below the triple-deck evolution problem associated with (1.3) is described. To the best of our knowledge, although the nonlinear unsteady triple-deck problem has been analysed by Smith (1979), Burggraf & Smith (1985), Duck (1985) and others in connection with lower-branch stability in attached boundary layers, the context of unsteady incipient separation and dynamic stall has not been seriously considered yet. A study of the linearized problem is undertaken in §3, together with various limiting solutions which lead to a study of the proposed nonlinear breakdown in §4. That is, we indicate that this new stage, defined by (1.3) and controlled by a nonlinear triple-deck problem, itself becomes singular within a finite time T . The breakdown of the new flow structure associated with this singularity leads on to yet another new stage, an Euler stage where the streamwise and lateral dimensions of the recirculating eddy both become comparable with the original boundary-layer thickness. That stage is a significant one, as it is likely to control the final emergence of the eddy from the boundary layer. Further remarks are presented in §5.

Before proceeding, we should make some additional comments here. The boundary-layer flow we are addressing is typically accelerated before being decelerated, and so from a linear point of view both Tollmien–Schlichting and Rayleigh modes can be present, the latter having neutral modes which come from the upper branch of the Tollmien–Schlichting modes at the pressure minimum upstream. In our present approach we are suppressing these modes, in a sense, or rather, we are suggesting that while they may be present it is our belief that the following account, one that is nonlinear in contrast to the above, could be the dominant process in dynamic stall. Also we wish to make it perfectly clear that our use of the term ‘breakdown’, above and below, refers to a breakdown of the equations obtained by taking the relevant scalings, and hence to a change in the flow structure. This is not necessarily different from the phenomenon of ‘bursting’ in other contexts. Indeed, bursting can be regarded as one particular example of breakdown as defined above.

2. The unsteady triple-deck problem

We consider first the classical stage (1.1 *a–d*), in which there is a sufficiently strong local adverse pressure gradient, prescribed by the quasi-steady outer inviscid solution, to force the classical non-interacting boundary layer to nearly separate, at some position $x = x_c$. At this position the boundary-layer solution has the well-known Goldstein (1948) singular form, with the tangential velocity profile at separation $u = U_0(y)$ having the behaviour

$$U_0(y) \sim \mu \frac{y^2}{2!} \quad \text{as } y \rightarrow 0+, \quad U_0(y) \rightarrow U_e(x_c) \quad \text{as } y \rightarrow \infty. \quad (2.1)$$

Here the constant $\mu > 0$ is the quasi-steady adverse pressure gradient at $x = x_c$. Stewartson (1970) considered the steady form of (1.1 *a–d*) and showed that the Goldstein singularity is not removable using triple-deck arguments, implying that

the triple deck is not the controlling agency for boundary-layer separation. In fact the triple-deck structure does control breakaway separation, and it is the inviscid outer solution that switches to an alternative form. However, if we concern ourselves with weak Goldstein singularities, where the separation is confined to the boundary layer, then modification of Stewartson's original analysis leads to the study of weak or marginal separations for both the steady (Stewartson *et al.* 1982) and unsteady case (Smith 1982). From the following work we contend, however, that the unsteady nonlinear triple deck is the controlling agency for far stronger separations.

Consider now the fully nonlinear unsteady triple-deck problem near separation. For a nonlinear-unsteady-viscous balance of forces in the boundary layer, the orderings $p = O(u^2)$, $u = O[(x_c - x)/y^2]$, $y = O(t^{\frac{1}{2}})$ are required, while the form of the separation profile (2.1) as $y \rightarrow 0+$ demands that $u = O[(x_c - x)^{\frac{1}{2}}]$, $p = O[(x_c - x)]$, $y = O[(x_c - x)^{\frac{1}{2}}]$, $t = O[(x_c - x)^{\frac{1}{2}}]$, the first three of which are the scalings obtained by Goldstein (1948) and Stewartson (1970). If most of the boundary layer is assumed to be simply displaced, riding over this viscous layer, then the perturbation to the separation profile, $u = U_0(y)$, is $O[(x_c - x)^{\frac{1}{2}}]$, and this gives rise to a normal velocity $O[R_1^{-\frac{1}{2}}(x_c - x)^{-\frac{1}{2}}]$ at the edge of the boundary layer. Hence as the position $x = x_c$ is approached the assumptions of classical boundary-layer theory (e.g. in (1.1)) break down. In order that a consistent interactive structure may be constructed, to smooth out this singular behaviour, the pressure induced by this normal velocity, necessarily of the same magnitude, must be comparable with that needed to drive the viscous sublayer. This occurs when $x_c - x = O(R_1^{-\frac{2}{3}})$, and it implies that we take $x - x_c = R_1^{-\frac{2}{3}}X$, $n = R_1^{-\frac{1}{3}}y = R_1^{-\frac{1}{3}}Y$, $t = R_1^{-\frac{1}{3}}T$, for the viscous sublayer, together with $\psi = R_1^{-\frac{2}{3}}\Psi$, $u = R_1^{-\frac{1}{3}}U$, $p = R_1^{-\frac{2}{3}}P$ and a displacement of the form

$$\delta^*(x, t) = R_1^{-\frac{1}{3}}[\delta_0 - R_1^{-\frac{1}{3}}A(X, T) + \dots]. \tag{2.2}$$

Thus we recover the orderings (1.3). The result of the above triple-deck interaction is to reduce the unsteady separation process to that of solving the following nonlinear evolution problem. We have the boundary-layer equations

$$U = \frac{\partial U}{\partial Y}, \quad \frac{\partial U}{\partial T} + U \frac{\partial U}{\partial X} - \frac{\partial \Psi}{\partial X} \frac{\partial U}{\partial Y} = - \frac{\partial P}{\partial X}(X, T) + \frac{\partial^2 U}{\partial Y^2}, \tag{2.3a, b}$$

subject to the following conditions:

$$U = \Psi = 0 \quad \text{on } Y = 0, \tag{2.3c}$$

$$\Psi \sim \frac{1}{6}\mu[Y + A(X, T)]^3 + \dots \quad \text{as } Y \rightarrow \infty, \tag{2.3d}$$

$$U \rightarrow \frac{1}{2}\mu Y^2, \quad \frac{\partial P}{\partial X} \rightarrow \mu \quad \text{as } |x| \rightarrow \infty, \tag{2.3e}$$

$$\frac{\partial P}{\partial X}(X, T) = \frac{1}{\pi} \int_{-\infty}^{\infty} \frac{\partial^2 A}{\partial \xi^2}(\xi, T) \frac{d\xi}{(X - \xi)}. \tag{2.3f}$$

The above conditions are, respectively, those of no-slip at the surface, the matching of the viscous flow to the displaced inviscid rotational flow, the matching to the attached boundary-layer flows upstream and downstream, and finally there is the usual subsonic pressure-displacement relation due to the outermost potential-flow region, the bar indicating that we take the Cauchy principal value.

Support for the view that the above structure is indeed the next stage on from that of Smith's can be obtained by recovering the latter's solution as our present time

$T \rightarrow -\infty$. If we write $X = |T|^{\frac{1}{2}}\hat{X}$, $Y = |T|^{\frac{1}{2}}\hat{Y}$ for $T \rightarrow -\infty$, with $A \sim |T|^{-\frac{1}{2}}\hat{A}_0(\hat{X})$, then the viscous flow in (2.3) has the starting form, as $T \rightarrow -\infty$,

$$\left. \begin{aligned} \Psi &= |T|^{\frac{1}{2}}[\frac{1}{2}\mu \hat{Y}^3 + |T|^{-\frac{1}{2}}\mu \hat{A}_0(\hat{X}) \hat{Y}^2 + |T|^{-\frac{1}{2}}\Psi(\hat{X}, \hat{Y}) + \dots], \\ U &= |T|^{\frac{1}{2}}[\frac{1}{2}\mu \hat{Y}^2 + |T|^{-\frac{1}{2}}\mu \hat{A}_0(\hat{X}) \hat{Y} + |T|^{-\frac{1}{2}}\hat{U}(\hat{X}, \hat{Y}) + \dots], \\ P &= |T|^{\frac{1}{2}}[\mu \hat{X} + 0 + |T|^{-\frac{1}{2}}\hat{P}_0(\hat{X}) + \dots], \end{aligned} \right\} \quad (2.4)$$

where the perturbation effects $\hat{\Psi}$, $\hat{U} = \partial\hat{\Psi}/\partial\hat{Y}$, \hat{P}_0 , \hat{A}_0 are governed by

$$\frac{\partial^3 \hat{\Psi}}{\partial \hat{Y}^3} - \mu \left[\frac{1}{2} \hat{Y}^2 \frac{\partial^2 \hat{\Psi}}{\partial \hat{Y} \partial \hat{X}} - \hat{Y} \frac{\partial \hat{\Psi}}{\partial \hat{X}} \right] = -\frac{d\hat{P}_0}{d\hat{X}} + \frac{1}{2}\mu \hat{A}_0 \frac{d\hat{A}_0}{d\hat{X}} \hat{Y}^2 + \frac{3}{2}\mu \left[\hat{A}_0 + \frac{2}{3}\hat{X} \frac{d\hat{A}_0}{d\hat{X}} \right] \hat{Y}$$

subject to the conditions of no-slip, the linear growth with \hat{Y} of $\hat{\Psi}$ at the outer boundary and with the usual steady subsonic relationship between \hat{A}_0 and \hat{P}_0 .

From Stewartson (1970), this problem can be reduced to the solution of a nonlinear integro-differential equation, which in a suitably normalized form is given by

$$\hat{A}_0^2(\hat{X}) = \int_{\hat{X}}^{\infty} \frac{d^2 \hat{A}_0}{d\xi^2} \frac{d\xi}{(\xi - \hat{X})^{\frac{1}{2}}} - \frac{2}{3} \int_{-\infty}^{\hat{X}} \left[\hat{A}_0 + \frac{2}{3}\xi \frac{d\hat{A}_0}{d\xi} \right] \frac{d\xi}{(\hat{X} - \xi)^{\frac{1}{2}}}, \quad (2.5)$$

subject to the upstream and downstream constraints

$$\hat{A}_0 \sim \begin{cases} c_1^+ \hat{X}^{-\frac{1}{2}} + c_2^+ \hat{X}^{-\frac{1}{2}} & \text{as } \hat{X} \rightarrow \infty, \\ c_1^- |\hat{X}|^{-\frac{1}{2}} + c_2^- |\hat{X}|^{-\frac{1}{2}} & \text{as } \hat{X} \rightarrow -\infty, \end{cases}$$

where c_1^\pm , c_2^\pm are unknown constants. Smith (1982) showed that (2.5) is the terminal form of (1.2). Smith did not solve this nonlinear equation, necessarily a numerical task, but instead indicated the nature of the solution by solving the linearized form

$$\int_{\hat{X}}^{\infty} \frac{d^2 \hat{A}_0^*}{d\xi^2} \frac{d\xi}{(\xi - \hat{X})^{\frac{1}{2}}} = \frac{2}{3} \int_{-\infty}^{\hat{X}} \left[\hat{A}_0^* + \frac{2}{3}\xi \frac{d\hat{A}_0^*}{d\xi} \right] \frac{d\xi}{(\hat{X} - \xi)^{\frac{1}{2}}}, \quad (2.6)$$

where formally $\hat{A}_0 = \epsilon \hat{A}_0^* + O(\epsilon^2)$ and $\epsilon > 0$ is small. Equation (2.6) then has the acceptable solution

$$\hat{A}_0^*(\hat{X}) = \text{Re} \int_0^{\infty} (a_0 + ia_1) r^{\frac{1}{2}} \exp \left[\frac{\pi^{\frac{1}{2}}}{\Gamma(\frac{3}{4})} \exp(\frac{2}{3}\pi i) r^{\frac{1}{2}} - ir\hat{X} \right] dr, \quad (2.7)$$

where Re denotes that we take the real part of the integral and a_0 and a_1 are undetermined constants. In addition it can be seen that when $|T| = O(R_1^{\frac{2}{10}})$ we recover Smith's scalings. The above tends to confirm that the origins of dynamic stall move on from the interactive marginal separation structure of Smith (1982) to the present full triple-deck problem (2.3a-f).

It was our original intention to solve (2.3a-f) numerically, marching forward in time from some initial point T_s ($(-T_s) \gg 1$) with the initial profile given by (2.4), and $A = |T_s|^{-\frac{1}{2}}\hat{A}_0$, where \hat{A}_0 is given by solving (2.5) numerically. However, initial computing trials using arbitrary starting profiles for A , with suitably decaying asymptotic behaviour, gave us cause for concern. The numerical approach adopted was as follows. First μ was set equal to unity (without loss of generality) and a guess was made for the local displacement $-A$. To start the calculation (2.3a-f) was solved using the Keller-box scheme applied in the classical inverse manner keeping A fixed, suppressing the Cauchy-Hilbert integral (2.3f) and neglecting all derivatives with respect to the time T . The transformation $X = \tan X_1$ was taken, with a uniform step-size DX_1 in X_1 , together with windward differencing, to account for the infinite domain and reversed flow respectively. Multiple sweeping of the streamwise direction

then led to a converged solution to the above which was then used as the 'initial-value' for the problem (2.3*a-f*). The equations were then marched forward in uniform increments DT of time. Typically we solved for the solution at the time level $T = T^* + \frac{1}{2}DT$, with the solution known at $T = T^*$, in an explicit first-order-accurate manner. Second-order accuracy for the solution at $T = T^* + DT$ was then obtained by extrapolation from the solution at times $T = T^*$ and $T = T^* + \frac{1}{2}DT$. Once again, windward differencing was used and so multiple sweeping was necessary to achieve convergence. As a check, the zigzag scheme (Telionis 1981) was also used. This scheme is second-order accurate in DT , but in order to satisfy the Courant–Friedrichs–Lewy criterion a restriction on the size of DT is necessary ($DT < \sec^2 X_1 DX_1 / U_{\max}$) and it is therefore not as robust.

A higher tolerance for convergence, typically 10^{-6} or 10^{-8} , was used to obtain the 'initial-value' solution and those at the first couple of time levels, whereas at subsequent time levels we took a tolerance of 10^{-4} or 10^{-6} . The step-size DX_1 took values $\pi/50$, $\pi/100$, $\pi/200$, while the values for the increment DT in time taken were 0.01, 0.005, 0.0025. Also the displacement was over-relaxed after each streamwise sweep, with a typical value of 1.2 for the over-relaxation parameter. In order to start the calculations the trial forms $A_1 = H(X^2 - \frac{1}{16}) / (X^2 + 1)^{\frac{3}{2}}$ and $A_2 = HX / (X^2 + 1)^2$ with $H = 0.5$ were taken. The first form, case 1, represents increasingly attached flow with a separation bubble followed by reattachment, while the second, case 2, represents increasingly reversed flow followed by reattachment. In both cases the decay far upstream and downstream allows the behaviour (2.3*e*). In all cases investigated a time was encountered where convergence was not achieved, with successive sweeps at the same time level leading to a divergent form.

Typical results obtained are given by figures 1–4. Initially there is a smooth development in the solution for the pressure P , skin-friction τ and local displacement $-A$. However, near a critical time there are major fluctuations in all these quantities especially as regards the skin friction, to a lesser extent the pressure, and to a minor extent the displacement. In figure 1(*a-c*) and figure 3(*a-c*) we have cases 1 and 2, respectively, where we have sketched the solution initially (or at the first couple of time levels) and near to the time where the calculations break down. This breakdown is due to the appearance of short-scale disturbances whose increasing amplification rates ultimately lead to non-convergence. In both cases the displacement changes only slightly, usually, with an increasing peak in A situated shortly after reattachment, followed by other minor oscillations. We also note a tendency of the original 'initial' disturbance to propagate downstream. This movement downstream is reflected in both the pressure and skin-friction results, while at the position corresponding to the peak in A there are extremely large oscillations in both the pressure and the skin friction. There is also the appearance of a wave-like disturbance upstream of these oscillations. Increasing the size of the initial disturbance (for example $H = 1.0$) did not seem to affect the results significantly, while the use of a finer grid in X_1 (figure 4*a-c*) resulted in the breakdown occurring roughly at the same time, although there appeared to be a lot more short-scale disturbances present. The use of a finer grid in time, however, dramatically altered the solution (figure 2*a-c*), with the time of breakdown advancing and the growth of the disturbances much enhanced. A representation of how breakdown occurs for case 1 is given by figure 5.

It was thought, at first, that the breakdown of the calculations might be due to the use of the incorrect starting condition, and that using the correct perturbation to the separating-flow form might ensure the continuation of the solution. However recent experience (Smith & Elliott 1985; Ryzhov & Smith 1984) has led us to expect

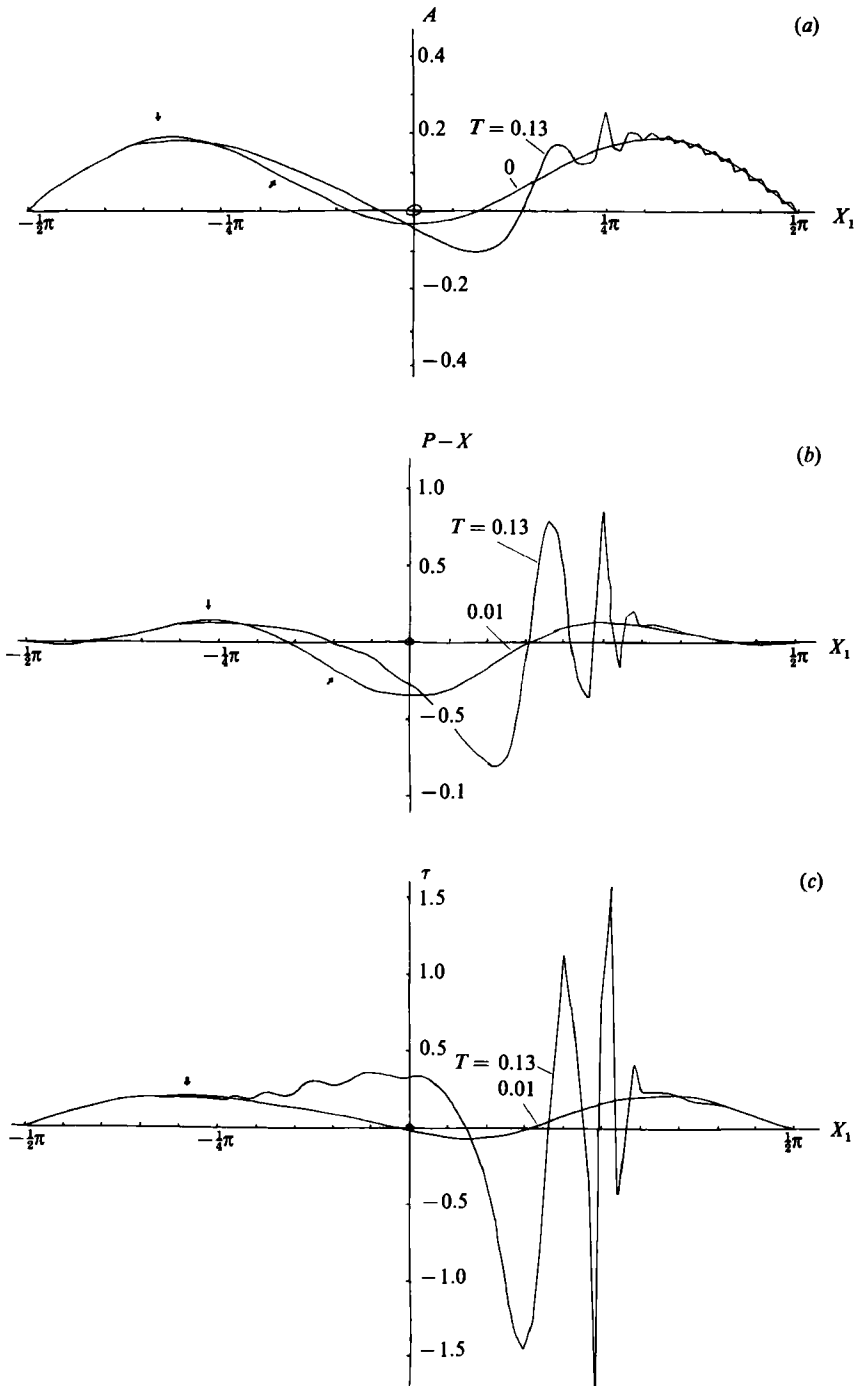


FIGURE 1. Results of nonlinear calculations (2.1 a-f) - case 1: initial displacement $A = H(X^2 - \frac{1}{16}) / (X^2 + 1)^{\frac{1}{2}}$ with $H = 0.5$, $DX_1 = \pi/100$, $DT = 0.01$. (a) The displacement $-A$, (b) the pressure perturbation $P - X$, (c) the skin friction τ .

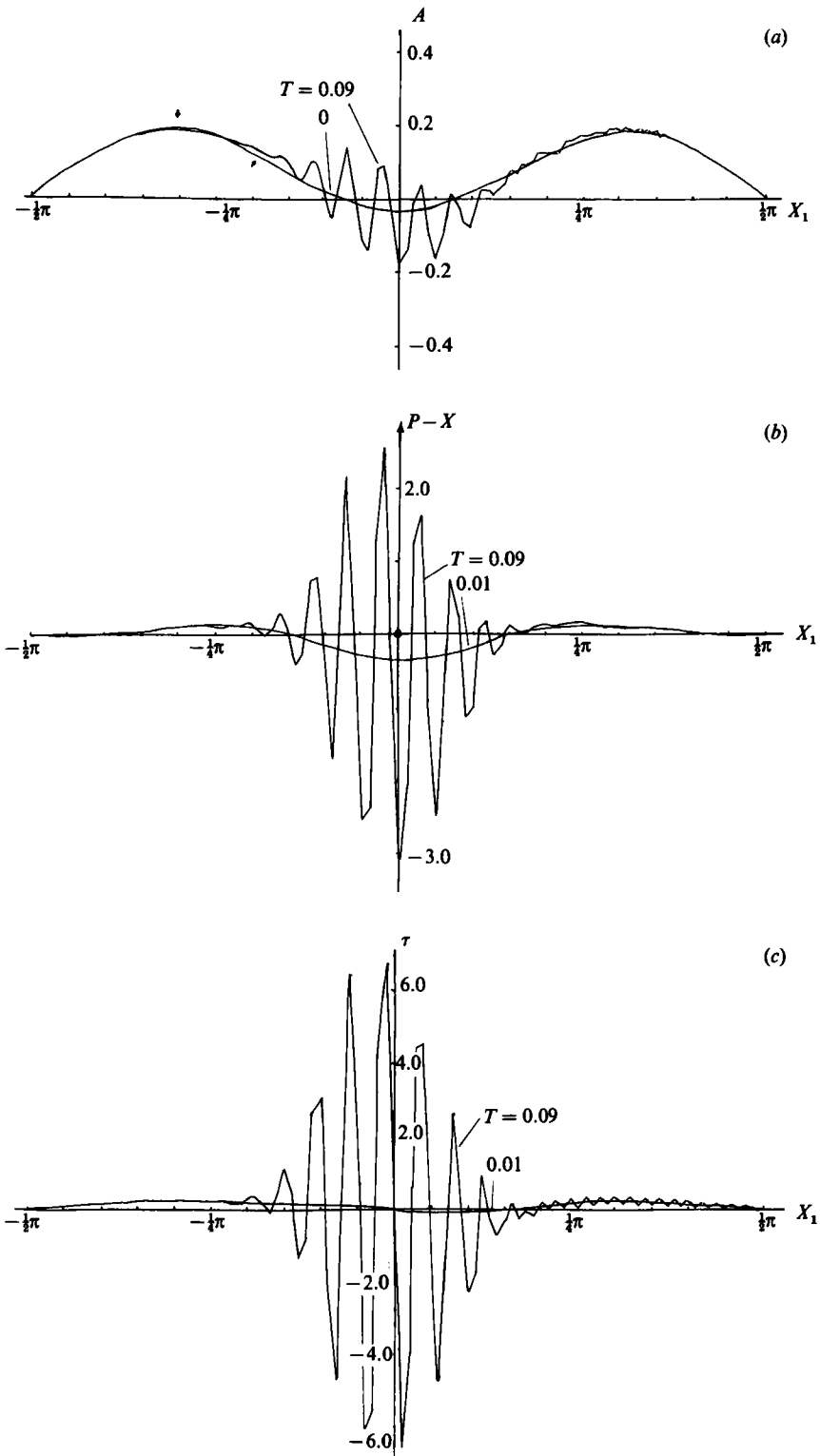


FIGURE 2. As for figure 1 but with $DT = 0.005$.

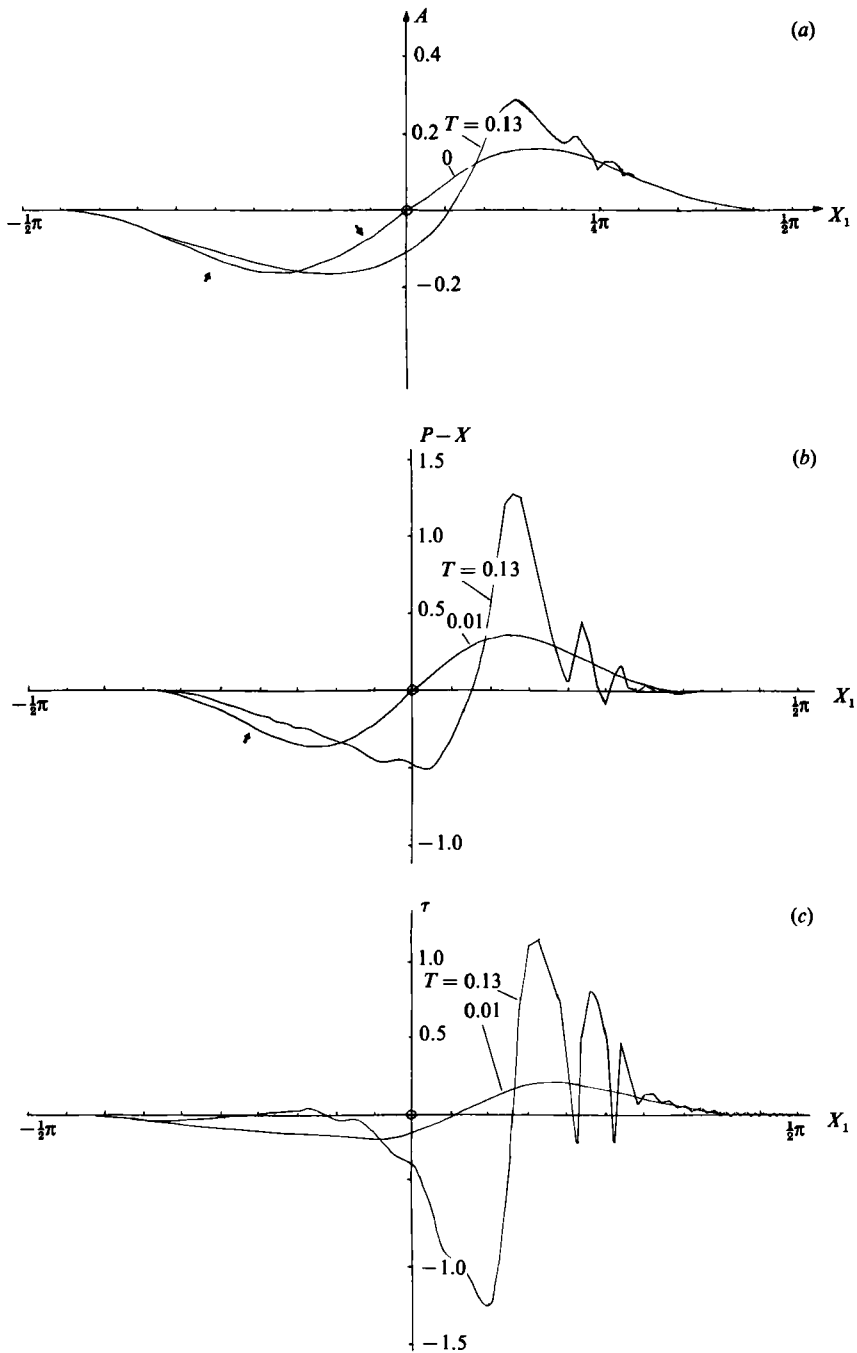


FIGURE 3. Results of nonlinear calculations (2.1 *a-f*)—case 2: initial displacement $A = HX/(X^2 + 1)^2$ with $H = 0.5$, $DX_1 = \pi/100$, $DT = 0.01$. (a) The displacement $-A$, (b) the pressure perturbation $P-X$, (c) the skin friction τ .

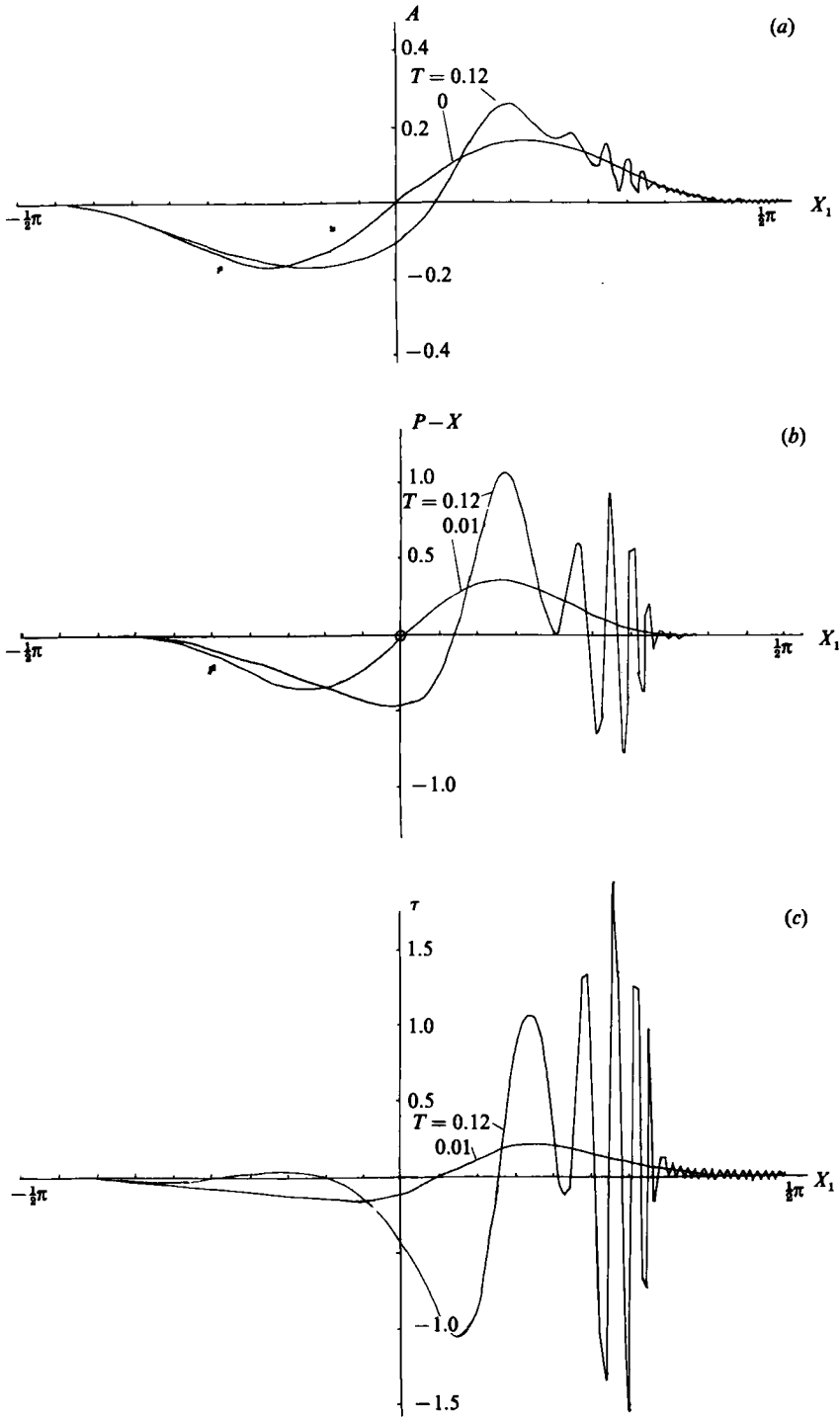


FIGURE 4. As for figure 3 but with $DX_1 = \pi/200$.

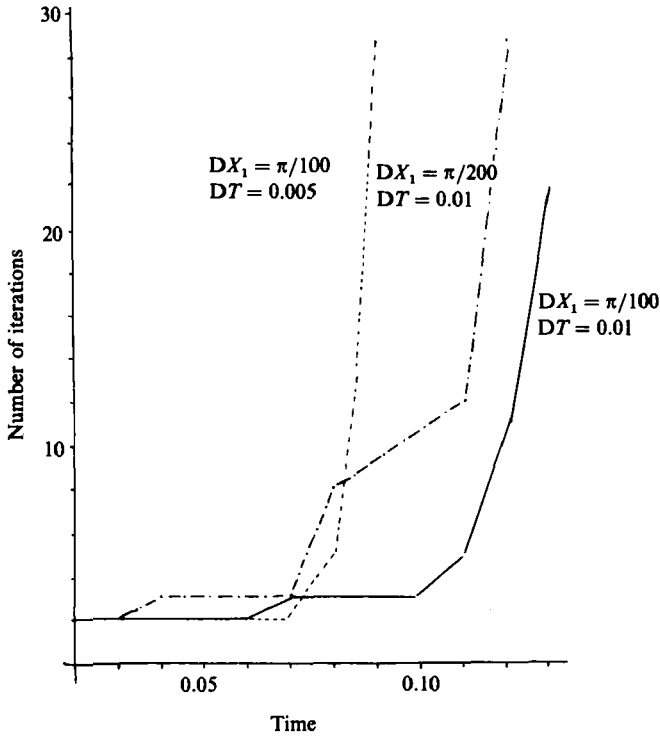


FIGURE 5. Schematic diagram of convergence for case 1.

a finite-time breakdown of (2.1 *a-f*) with the solution changing on small streamwise and fast time scales. In order to provide some firmer foundation, we decided that a numerical and analytical investigation of a linearized form of (2.3 *a-f*), with (2.7) as the starting form for *A*, could be useful, and this guide is presented in the following section.

3. The linearized problem

Given that the linearization in the previous stage is helpful in pointing to the nonlinear behaviour, and that the authors' recent work (Smith & Elliott 1985) on the corresponding unsteady classical problem was also aided by linear analysis, we follow a similar line here. To this end we write

$$[\Psi, U, P, A] = \mu[\frac{1}{6}Y^3, \frac{1}{2}Y^2, X, 0] + \epsilon[\Psi_L, U_L, P_L, A_L] + O(\epsilon^2)$$

where $0 < \epsilon \ll 1$. The linearized triple-deck form is then given by

$$U_L = \frac{\partial \Psi_L}{\partial Y}, \quad \frac{\partial U_L}{\partial T} + \mu \left[\frac{1}{2} Y^2 \frac{\partial U_L}{\partial X} - Y \frac{\partial \Psi_L}{\partial X} \right] = -\frac{\partial P_L}{\partial X} + \frac{\partial^2 U_L}{\partial Y^2}, \tag{3.1 a, b}$$

subject to the conditions

$$U_L = \Psi_L = 0 \quad \text{on } Y = 0, \tag{3.1 c}$$

$$(\Psi_L, U_L, P_L, A_L) \rightarrow (0, 0, 0, 0) \quad \text{as } |X| \rightarrow \infty, \tag{3.1 d}$$

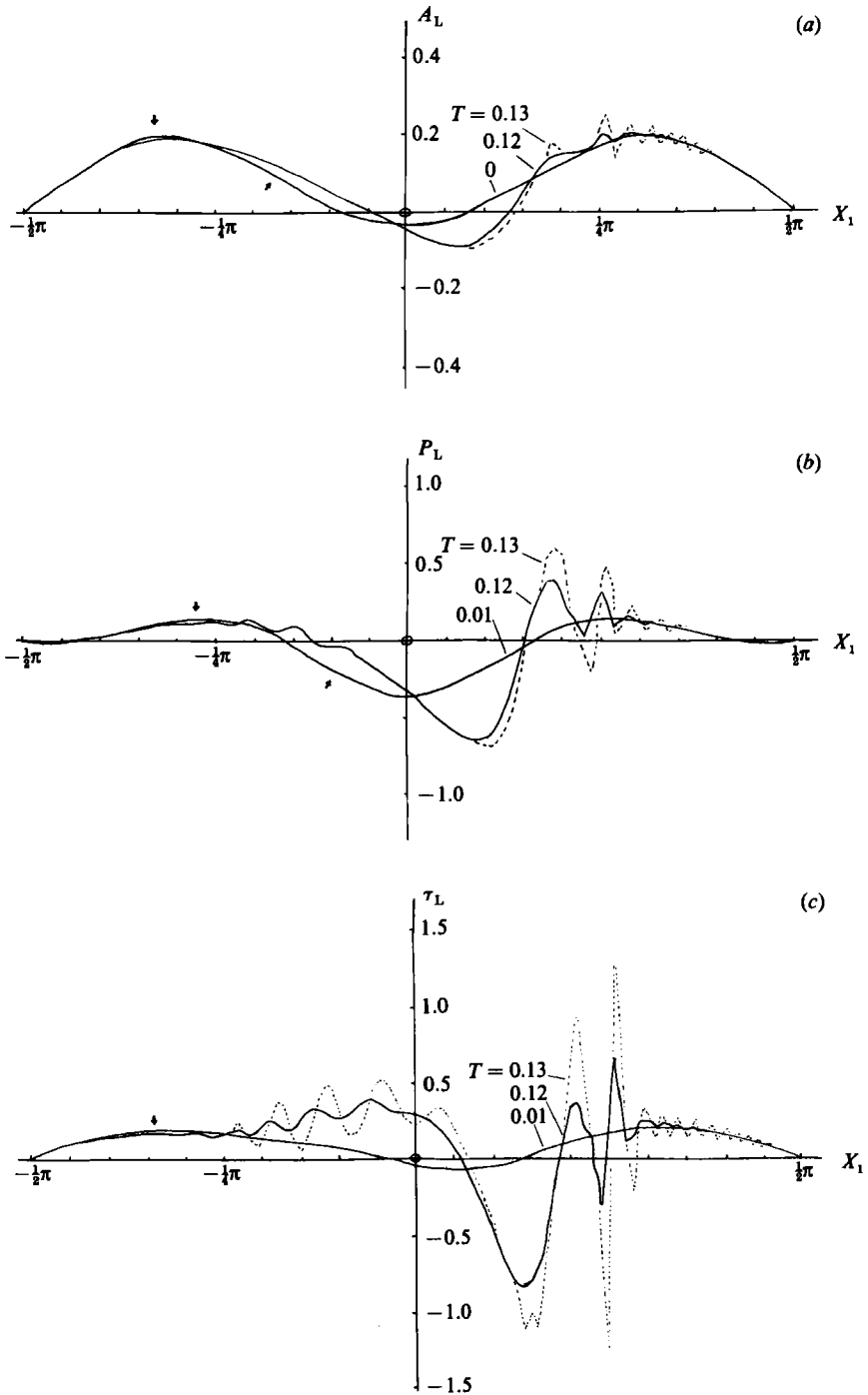


FIGURE 6. Results of linear calculations (3.1 a-f) - case 1: initial displacement $A_L = H(X^2 - \frac{1}{16}) / (X^2 + 1)^{\frac{1}{2}}$ with $H = 0.5$, $DX_1 = \pi/100$, $DT = 0.01$. (a) The displacement $-A_L$, (b) the pressure P_L , (c) the skin friction τ_L .

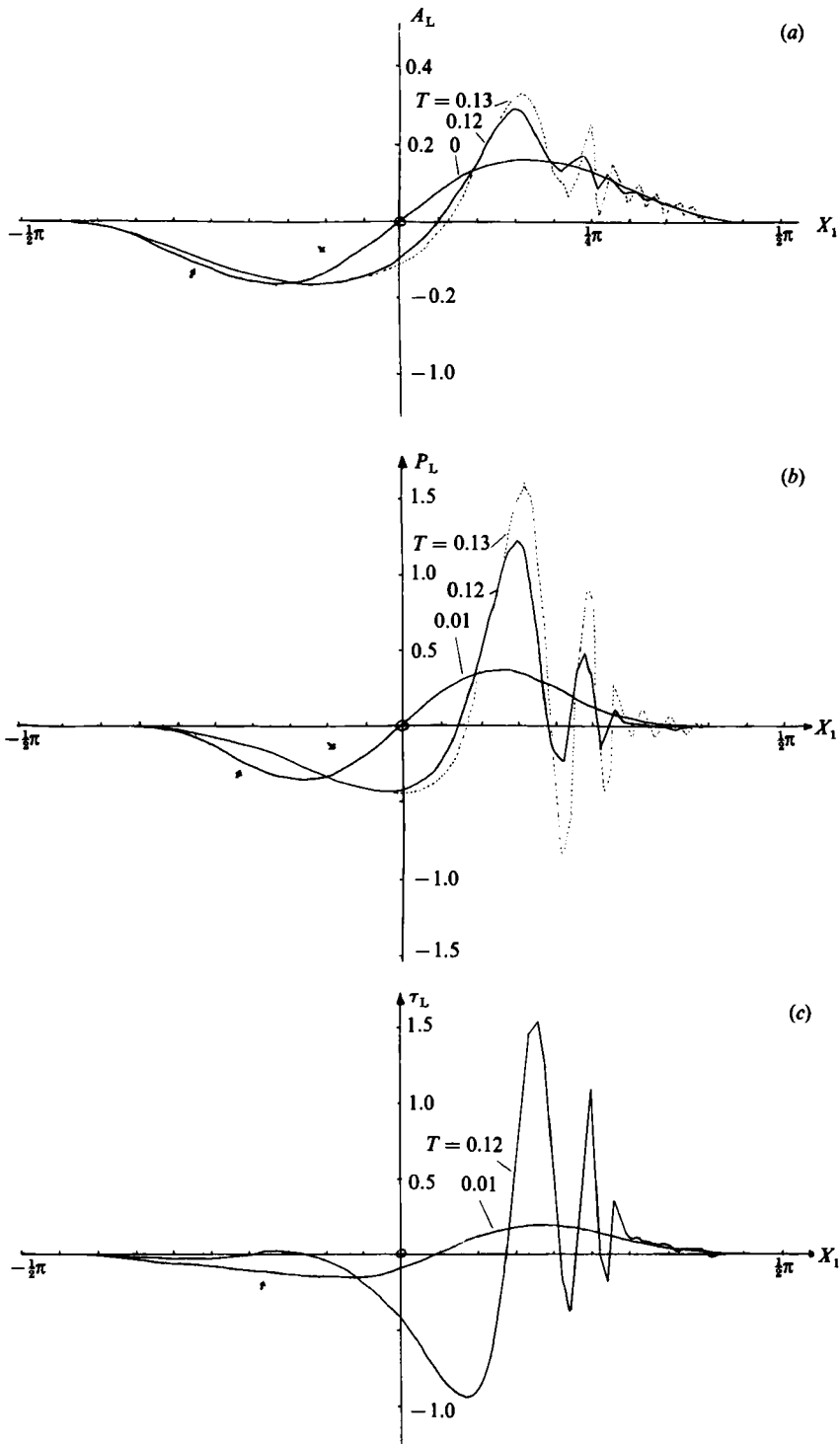


FIGURE 7. Results of linear calculations (3.1 a-f) - case 2: initial displacement $A_L = HX/(X^2 + 1)^2$ with $H = 0.5$, $DX_1 = \pi/100$, $DT = 0.01$. (a) The displacement $-A_L$, (b) the pressure P_L , (c) the skin friction τ_L .

together with the asymptotic form as $Y \rightarrow \infty$

$$\Psi_L \sim \mu A_L(X, T) \frac{Y^2}{2!} + \int_{-\infty}^X \frac{\partial A_L}{\partial T}(\xi, T) d\xi + \frac{2}{3\mu Y} P_L(X, T) \dots \tag{3.1e}$$

Here P_L and A_L are linked by the usual pressure-displacement relation, and it can be verified that as $T \rightarrow -\infty$ the form of (3.1a-e) takes on a behaviour similar to (2.4) with the leading-order skin-friction A_L being given by (2.7).

Because of the arbitrariness present in (2.7) it was decided to again use the trial forms $A_L = A_1$ and $A_L = A_2$, as given in the nonlinear case, to start the numerical calculation of (3.1a-e). The numerical method used was that as described for the nonlinear calculation with suitable modifications. Typical results for case 1 and case 2 are given by figure 6(a-c) and figure 7(a-c) respectively. Here $\tau_L = \partial U_L(X, 0) / \partial Y$. The results mirror those of the nonlinear calculations, with breakdown again due to the fast growth of small-scale disturbances. As before the smaller the lengthscale the faster the growth of the disturbance; however, the amplitudes of the disturbances are perhaps not quite as large as those given by the nonlinear calculations. Once again, it appears that there is a finite time breakdown, say as $T \rightarrow T_0^-$, of the solution to (3.1a-e). Our belief is that even if we used (2.7) to start our calculation the small-scale errors thrown up by the necessary discretization of the solution would grow and eventually terminate the calculations in a similar manner. To provide support for our belief an analytical investigation of (3.1a-e) is discussed below.

Let us first introduce the local wall shear

$$\lambda(X, T) = \left. \frac{\partial^2 \Psi_L}{\partial Y^2} \right|_{Y=0}$$

The solution to (3.1a-e) can be obtained formally by using a double Fourier transform in X and T . If we look for a solution of the form

$$\Psi_L(X, \xi, T) = \frac{1}{(2\pi)^2} \int_{-\infty}^{\infty} \int_{-\infty}^{\infty} \bar{\Psi}(\omega, \xi, \beta) \exp\{i[\omega X + \beta T]\} d\omega d\beta$$

and we take $Q(\omega, \xi, \beta) = \partial^2 \bar{\Psi} / \partial \xi^2$, where we have taken $\xi = (2i\omega\mu)^{1/2} Y^2$, then it can be shown that Q satisfies

$$\xi \frac{\partial^2 Q}{\partial \xi^2} + \frac{5}{2} \frac{\partial Q}{\partial \xi} + (k - \frac{1}{4}\xi) Q = -\frac{1}{4\sqrt{2}} \frac{1}{(2i\omega\mu)^{3/4}} \frac{1}{\xi^{3/4}} [i\omega \bar{P}(\omega, \beta)], \tag{3.2a}$$

where as $\xi \rightarrow 0$ we have the behaviour

$$Q \sim \frac{1}{2^{3/4} (2i\omega\mu)^{3/4} \xi^{3/4}} (i\omega) \bar{P}(\omega, \beta) - \frac{2}{3} \frac{k}{(2i\omega\mu)^{1/2}} \bar{\lambda}(\omega, \beta) + \dots, \tag{3.2b}$$

and although $Q = O(\xi^{-3/4})$ as $\xi \rightarrow \infty$ the relevant condition is

$$\int_0^{\infty} Q(\omega, \xi, \beta) d\xi = \frac{1}{(2i\omega\mu)^{3/4}} [\mu \bar{A}(\omega, \beta) - \bar{\lambda}(\omega, \beta)]. \tag{3.2c}$$

Here \bar{P} , \bar{A} and $\bar{\lambda}$ are the respective double transforms of P_L , A_L and λ while the parameter $k = -\frac{1}{2}i\beta / (2i\omega\mu)^{1/2}$ represents the relative influence of spatial to temporal scales. The solution to (3.2a-c) is best seen by taking

$$Q = \frac{1}{4\sqrt{2}} \frac{1}{(2i\omega\mu)^{3/4}} \frac{1}{\xi^{3/4}} [(i\omega) \bar{P}(\omega, \beta)] H(\xi, k),$$

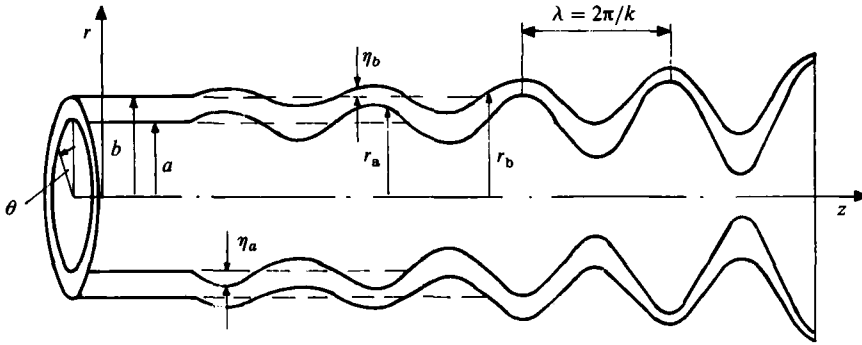


FIGURE 1. Schematic description of an unstable perturbation in an annular jet.

generalizations such as the inclusion of viscosity (Dombrowski & Johns 1963) or spreading (Weihs 1978) did not change the qualitative behaviour.

The annular jet is thus useful in showing how the different dominant modes of instability arise and change in importance as one changes the ratio of inner to outer radii of the annulus from the circular jet limit ($a/b \rightarrow 0$) to the ($a/b \rightarrow 1$) thin flat sheet case.

In the present paper we examine the linear stability of an infinitely long annular jet moving relative to the media external and internal to the jet. The stability of jet shape to temporal perturbations in the radius is studied, as there is no experimental evidence for the existence of the primary modes of spatial instability discussed by Keller, Rubinow & Tu (1973). A parametric study of the effects of surface tension, viscosity and relative velocity is performed.

2. Formulation of the stability problem

Consider an infinitely long liquid jet of annular cross-section with internal radius a , external radius b , and constant density ρ , viscosity μ and surface tension σ (see figure 1). The jet is moving at fixed axial velocity U through an inviscid medium of constant density $\hat{\rho}$ ($\hat{\rho} \ll \rho$).

The linear stability of this jet, when subjected to infinitesimal perturbations, will now be studied. Defining (figure 1) a cylindrical coordinate system (r, θ, z) in which the z -axis coincides with the jet axis and moves with it at speed U , one can write the perturbed form of the cylinder, assuming only axisymmetric perturbations, as

$$r_b(z, t) = b + \eta_b(z, t); \quad r_a(z, t) = a + \eta_a(z, t), \quad (1)$$

where $\eta_a, \eta_b \ll a, b$, respectively. The perturbations take the form

$$\eta_j(z, t) = \text{Re} (\eta_{0j} \exp(\beta_j t + ik_j z)) \quad (j = a, b), \quad (2)$$

where β_j are the complex frequencies and k_j the wavenumbers of the perturbations. Conservation of mass over a finite but arbitrary length of the jet much larger than the wavelength leads to the relations (Meyer 1983)

$$\beta_a = \beta_b = \beta; \quad k_a = k_b = k; \quad \frac{\eta_{0b}}{\eta_{0a}} = \frac{a}{b}, \quad (3)$$

when a/b is of order 1. This does not include the limiting case of a full cylinder ($a \rightarrow 0$) or a hollow jet (a finite, $b \rightarrow \infty$), but these cases do not require the compatibility

and hence $k \rightarrow 0$ corresponds to $T \rightarrow -\infty$ with the solution to (3.5a-c) matching that of Smith's.

What we really require, however, is the ultimate form of the solution, be it as T tends to a finite value or as $T \rightarrow +\infty$. This can be obtained by considering $|k| \gg 1$. For $|k|$ large the Appendix shows that to leading order (3.5a-c) becomes

$$-(\frac{1}{2}\pi)^{\frac{1}{2}} \frac{1}{|k|^{\frac{1}{2}}} \bar{P}(\omega, \beta) = -2^{\frac{1}{2}} \pi^{\frac{1}{2}} \mu^{\frac{1}{2}} \frac{k}{(i\omega)^{\frac{1}{2}}} \bar{A}(\omega, \beta), \tag{3.7a}$$

which, with the use of relation (2.3c), can be inverted to give the evolution equation, in an integro-differential form

$$\mu \frac{\partial A_L}{\partial T}(X, T) + 'O' = \frac{\mu^{\frac{1}{2}}}{2\sqrt{2}} \int_{-\infty}^T \left\{ \int_X^{\infty} \frac{\partial^2 A_L}{\partial \xi^2}(\xi, T') \frac{d\xi}{(\xi-X)^{\frac{1}{2}}} \right\} \frac{dT'}{(T-T')^{\frac{1}{2}}} \tag{3.7b}$$

for A_L , where the 'O' represents unknown terms at $T = -\infty$, $X = -\infty$ due to integration. We see that (3.7b) gives the possible scaling $|X - X_0| \sim |T - T_0|^{\frac{1}{2}}$, which is in line with $k \rightarrow \infty$ as $T \rightarrow T_0^-$ and implies a final form with this ordering. However (3.7b) is a little difficult to interpret directly. If, instead, we consider (3.7a) together with (3.4) we obtain the dispersion relation $\mu\beta^3 = \frac{1}{8}\pi^2\omega^5$. So if we take $P^*(\omega, T)$ where

$$P_L(X, T) = \frac{1}{2\pi} \int_{-\infty}^{\infty} P^*(\omega, T) \exp(i\omega X) d\omega,$$

then
$$P^*(\omega, T) = \sum_j B_j(\omega) \exp\left[\frac{1}{8} \frac{\pi^{\frac{1}{2}} \omega^{\frac{5}{2}}}{\mu^{\frac{1}{2}}} \exp(\frac{2}{3}\pi j i) T\right] \quad (j = 0, 1, 2).$$

It appears at first that there are three discrete modes, one stable ($j = 2$), one unstable ($j = 1$) and one neutral ($j = 0$); however further study implies that the neutral mode is not present (see §4). After a short time of exponential growth the unstable mode will dominate, giving

$$P_L \sim \frac{1}{2\pi} \int_0^{\infty} \{B_1(\omega) \exp\{i\omega[X - \frac{1}{4}(\pi\omega)^{\frac{1}{2}}T]\} + C.C\} \exp\left(\frac{\sqrt{3}}{4} \frac{\pi^{\frac{1}{2}} \omega^{\frac{5}{2}}}{\mu^{\frac{1}{2}}} T\right) d\omega,$$

where C.C denotes the complex conjugate. Hence for a particular wavenumber, say ω_0 , the unstable mode grows exponentially and moves downstream with wavespeed $\frac{1}{4}(\pi\omega_0)^{\frac{1}{2}}/\mu^{\frac{1}{2}}$.

It can be seen next that the above gives strong evidence of a breakdown. For even if we choose $B_1(\omega)$ so that the integrand is well-behaved, having exponentially decaying behaviour as $|\omega| \rightarrow \infty$ in the form

$$P^*(\omega, T) = \exp\left[\frac{1}{4} \frac{\pi^{\frac{1}{2}} \omega^{\frac{5}{2}}}{\mu^{\frac{1}{2}}} e^{2\pi i/3} (T - T_0)\right] + \dots,$$

where T_0 is some constant, then, although the solution is initially well-behaved, as $T \rightarrow -\infty$, there is a breakdown as $T \rightarrow T_0^-$. Thus we have indicated formally the possibility of breakdown, whose form we could presumably obtain from the evolution equation (3.7), and the analysis seems to suggest that the linear triple-deck problem suffers a finite-time collapse. We see from the solution for P^* that the larger the value of ω , i.e. the smaller the X -scale of the disturbance, the faster the exponential growth.

The property above, that the smaller the lengthscale of a disturbance the faster is its growth, tends to back up the numerical findings described earlier, although it must by the same token cast doubt on the accuracy of those numerical solutions. Necessarily, small errors caused by discretization of the equations are also magnified

by the above instability. Refining the grid does not improve the situation, since it allows smaller-wavelength disturbances to be resolved and so results in more rapidly growing instabilities. We believe that the dominant phenomenon can still entail a finite-time breakdown of the solution to (3.1*a-e*) due to such small-scale growth. It may well be that nonlinearity would smooth out the small-scale growth and allow the solution to continue past $T = T_0$. The earlier nonlinear calculations seem, however, to indicate otherwise and we feel that the nonlinear problem mirrors the above, resulting in a finite-time breakdown at $T = T_0$ about a position $X = X_0$ with $|X - X_0| \sim (T_0 - T)^{\frac{1}{2}}$. That is followed through in §4.

The breakdown of such a linear solution was noted also by Moore (1979) while studying Kelvin-Helmholtz instabilities on velocity-discontinuity shear layers. There, as here, the development of a finite-time singularity occurs because the scalings chosen are not valid for sufficiently small-scale disturbances. If, however, the wavenumber spectrum of the initial disturbance is made to decay sufficiently rapidly as $|\omega| \rightarrow \infty$ then initial-value problems for larger-scale disturbances can be accommodated (Moore 1979; Ryzhov & Smith 1984). Similar remarks hold for our linearized problem above. If the complete spectrum is considered, the linear disturbances do *not* exhibit temporal growth at infinite wavenumber and therefore they exhibit no finite-time breakdown then. The breakdown we postulate above is because we are dealing with approximate solutions (for R_1 large) valid for a certain wavenumber range.

4. The finite-time breakdown

To provide evidence for a *nonlinear* breakdown let us look for a consistent description to (2.3*a-f*), assuming that A becomes large. From the asymptote (2.3*c*) we see that, for Y large, $Y = O(A)$ and hence $\Psi = (A^3)$, $U = O(A^2)$. A balancing of the unsteady, inertial and pressure forces then gives the scalings $P = O(A^4)$, $|X| = O(A^{-3})$ and $|T| = O(A^{-5})$. However, we cannot balance the $O(1)$ viscous term, which is much smaller than the other terms. Therefore, to leading order, we have an inviscid structure with a fast timescale and lengthscales $|X| \sim |T|^{\frac{1}{2}}$, $Y \sim |T|^{-\frac{1}{2}}$ producing a 'bursting' effect as $T \rightarrow 0^-$. The problem is given now by

$$U = \frac{\partial \Psi}{\partial Y}, \quad \frac{\partial U}{\partial T} + U \frac{\partial U}{\partial X} - \frac{\partial \Psi}{\partial X} \frac{\partial U}{\partial Y} = -\frac{\partial P}{\partial X}(X, T), \quad (4.1 a, b)$$

subject to the inviscid constraint of tangential flow

$$\Psi = O(Y) \quad \text{as } Y \rightarrow 0 \quad (4.1 c)$$

and, as $Y \rightarrow \infty$, the asymptote

$$\Psi \sim \frac{1}{6} [Y + A(X, T)]^3 + \int_{-\infty}^X \frac{\partial A}{\partial T}(\xi, \mu T) d\xi + \frac{2}{3Y} P(X, T) + \dots \quad (4.1 d)$$

and the pressure-displacement law (2.3*f*). The above problem holds so long as a thin viscous sublayer of thickness $O(A^{-\frac{1}{2}})$ exists in which the skin friction is $O(A^{\frac{1}{2}})$, which is large on the present scalings. Thus there is the continuing increase of reversed flow associated with A increasing, continuing the process of Smith (1982), although now, of course, the link is not so obvious. The existence of the viscous sublayer, necessary to bring the inviscid slip velocity to rest, is a real factor. Van Dommelen (1981) and Elliott *et al.* (1983) have shown that unsteady classical viscous layers are prone to

eruptions, causing a breakdown themselves. Let us assume for now, however, that the form of A allows the attached viscous layer to exist.

The same arguments apply to the linear triple-deck problem (3.1 *a-e*) and this also results in an inviscid problem for a region where $Y = O(A^q) \gg 1$. Here q is an unknown positive constant. In this region we have $\Psi = O(A^{1+2q})$, $U = O(A^{1+q})$, $P = O(A^{1+3q})$, $|X| = O(A^{-3q})$, $|T| = O(A^{-5q})$ and the resulting problem is given by the linearization of (4.1 *a-d*). Again we require a viscous sublayer whose thickness is of $O(A^{-5q/2})$ which gives rise to a skin friction of $O(A^{1+7q/2})$. We note that once again we have $|X| \sim |T|^{\frac{2}{3}}$, $Y \sim |T|^{-\frac{1}{3}}$. The transformed linear problem is then given by

$$\left(\frac{1}{2}Y^2 \pm \frac{\beta}{|\omega|}\right) \frac{\partial \bar{\Psi}}{\partial Y} - Y\bar{\Psi} = -\bar{P}$$

subject to $\bar{\Psi} = 0$ on $Y = 0$ and having the behaviour

$$\bar{\Psi} \sim \left(\frac{1}{2}Y^2 \pm \frac{\beta}{|\omega|}\right) \bar{A}(\omega, \beta) \quad \text{as } Y \rightarrow \infty,$$

where as before $\bar{P} = |\omega|\bar{A}$. Here the \pm sign is taken for $\omega \gtrless 0$. it can easily be seen that $\bar{\Psi}$ has the solution

$$\bar{\Psi} = -4\bar{P} \left\{ \left(\frac{1}{2}Y^2 \pm \frac{\beta}{|\omega|}\right) \int_0^Y \frac{dY_1}{(Y_1^2 \pm 2\beta/|\omega|)^2} \right\},$$

which, on using the asymptotic condition, leads to the result

$$\bar{P} \int_0^\infty \frac{dY_1}{(Y_1^2 \pm 2\beta/|\omega|)^2} = -\frac{1}{4}\bar{A}.$$

If we consider the case $\omega \geq 0$ only, then it is clear that for β -real there is no solution, but for β -complex we have

$$\mp \frac{i\pi}{(-2\beta/|\omega|)^{\frac{3}{2}}} \bar{P} = -\bar{A},$$

where now the \mp sign refers to $\text{Im}(-2\beta/\omega) \gtrless 0$. Thus using $\bar{P} = |\omega|\bar{A}$ we are led to two relations which square up to give the single dispersion relation $8\beta^3 = \pi^2|\omega|^5$ as in §3, but we must insist that β is not real. The same result is found for $\omega < 0$. Alternatively we have the relation

$$(i\beta)^{\frac{2}{3}}\bar{A}(\omega, \beta) = -\frac{\pi}{2\sqrt{2}}(i\omega)^{\frac{1}{3}}\bar{P}(\omega, \beta),$$

which is of course the result (3.7 *a*), the asymptotic form as $|k| \rightarrow \infty$ of the linear triple-deck problem of §3. Hence the above consistent description seems to tie in with our previous linear analysis.

What we require is the terminal form of the nonlinear and linear triple-deck problems as $T \rightarrow T_0^-$. Let us take the scales $X - X_0 = (T_0 - T)^{\frac{1}{2}}\bar{X}$ and $Y = (T_0 - T)^{-\frac{1}{2}}\bar{Y}$ with $\Psi = (T_0 - T)^{-\frac{1}{2}-s}\bar{\Psi}(\bar{X}, \bar{Y})$, $U = (T_0 - T)^{-\frac{1}{2}-s}\bar{U}(\bar{X}, \bar{Y})$, $A = (T_0 - T)^{-s}\bar{A}(\bar{X})$, $P = (T_0 - T)^{-\frac{1}{2}-s}\bar{P}(\bar{X})$, where $s = \frac{1}{5}$ for the nonlinear problem and an unknown positive constant for the linear problem ($A = A_L, \dots$ etc). We obtain, for the case of the nonlinear problem,

$$\bar{U} = \frac{\partial \bar{\Psi}}{\partial \bar{Y}}, \quad \frac{1}{5} \left[(1+5s)\bar{U} + 3\bar{X} \frac{\partial \bar{U}}{\partial \bar{X}} - \bar{Y} \frac{\partial \bar{U}}{\partial \bar{Y}} \right] + \bar{U} \frac{\partial \bar{U}}{\partial \bar{X}} - \frac{\partial \bar{\Psi}}{\partial \bar{X}} \frac{\partial \bar{U}}{\partial \bar{Y}} = -\frac{d\bar{P}}{d\bar{X}} \quad (4.2a, b)$$

subject to the inviscid tangential flow constraint and the matching asymptote obtained from (4.1 *c, d*). Elliott *et al.* (1983) solved a somewhat similar problem

without the unknown pressure gradient, but the method of characteristics used in that problem does not seem to be able to resolve the present one. The above is, of course, subject to the corresponding sublayer-similarity problem (where $Y = O[(T_0 - T)^{\frac{1}{2}}]$) having a solution. We may, however, linearize (4.2*a, b*) to obtain the equations

$$\tilde{U} = \frac{\partial \tilde{\Psi}}{\partial \tilde{Y}}, \quad \frac{1}{5} \left[(1 + 5s) \tilde{U} + 3\tilde{X} \frac{\partial \tilde{U}}{\partial \tilde{X}} - \tilde{Y} \frac{\partial \tilde{U}}{\partial \tilde{Y}} \right] + \frac{1}{2} \tilde{Y}^2 \frac{\partial \tilde{U}}{\partial \tilde{X}} - \tilde{Y} \frac{\partial \tilde{\Psi}}{\partial \tilde{X}} = -\frac{d\tilde{P}}{d\tilde{X}} \quad (4.3a, b)$$

which are subject to the conditions

$$\tilde{\Psi} = O(\tilde{Y}) \quad \text{as } \tilde{Y} \rightarrow 0, \quad \tilde{\Psi} \sim \frac{1}{2} \tilde{A}(\tilde{X}) \tilde{Y}^2 \quad \text{as } \tilde{Y} \rightarrow \infty. \quad (4.3c)$$

Here the linearized-nonlinear case has $s = \frac{1}{5}$, while $s > 0$ for the general linear case. We may solve (4.3*a-c*) by again introducing $z = \tilde{Y}^2$ and $\tilde{Q}(\tilde{X}, z) = \partial^2 \tilde{\Psi} / \partial z^2$, and we find that \tilde{Q} has to satisfy

$$\frac{2}{5} \left[(5s - 2) \tilde{Q} + 3\tilde{X} \frac{\partial \tilde{Q}}{\partial \tilde{X}} - 2z \frac{\partial \tilde{Q}}{\partial z} \right] + z \frac{\partial \tilde{Q}}{\partial \tilde{X}} = \frac{1}{2z^{\frac{3}{2}}} \frac{d\tilde{P}}{d\tilde{X}},$$

where the term in the square brackets comes from the unsteady effects. These are subject to the constraints

$$\tilde{Q} = 0 \left(\frac{1}{4z^{\frac{3}{2}}} \right) \quad \text{as } z \rightarrow 0,$$

$$\tilde{Q} \rightarrow 0 \quad \text{as } z \rightarrow \infty,$$

$$\int_0^\infty \tilde{Q} dz = \frac{1}{2} \tilde{A}(\tilde{X}).$$

We can simplify the problem by eliminating the term $\tilde{X} \partial \tilde{Q} / \partial \tilde{X}$. If we introduce the new variable

$$\xi = z^{\frac{1}{2}} \tilde{X} = \tilde{Y}^3 \tilde{X} = Y^3 X$$

and take $\tilde{Q} = \tilde{Q}(\xi, z)$ and $\tilde{P} = \tilde{P}(\xi, z)$ we find that

$$z \frac{\partial \tilde{Q}}{\partial z} + \frac{1}{2} \left[(2 - 5s) \tilde{Q} - \frac{1}{2} z^{\frac{1}{2}} \frac{\partial \tilde{Q}}{\partial \xi} \right] = -\frac{5}{8} \frac{\partial \tilde{P}}{\partial \xi}.$$

If we now take the Fourier transform of this equation with respect to $\xi (\xi \rightarrow \omega)$ we find that

$$z^{5s/2} \exp \left[\frac{1}{2} i \omega z^{\frac{1}{2}} \right] \frac{\partial}{\partial z} \left(z^{1-5s/2} \exp \left[-\frac{1}{2} i \omega z^{\frac{1}{2}} \right] Q^*(\omega, z) \right) = -\frac{5}{8} (i \omega) P^*(\omega, z), \quad (4.4)$$

where Q^* and P^* are the respective transforms of \tilde{Q} and \tilde{P} . It can be seen that there is a formal solution for Q^* and this tends to back up our belief in the existence of a finite-time singularity. So far, however, no solution has been obtained from the conditions to give the terminal form for P (or alternatively for A) and this is certainly something one would wish to obtain. It is also in contrast to the simple solution to (4.1*a, b*) for the shear-flow case in Burggraf & Smith (1985), where the large-amplitude form for A satisfies a Benjamin-Ono equation, although again the possibility of a finite-time singularity in the shear-flow case, with a less simple form for A , seems to us a strong one.

Given that the breakdown does occur in the present nonlinear and linear cases, what is the next structure to govern the flow? According to the preceding analysis there is a short-scale breakdown with $|X - X_0| \sim |T - T_0|^{\frac{1}{2}}$ and with the viscous flow splitting into two. We have an outer inviscid part, erupting like $Y \sim |T - T_0|^{-\frac{1}{2}}$, and

a diminishing inner viscous region with $Y \sim |T - T_0|^{\frac{1}{2}}$. We see that eventually this outer region will be indistinguishable from the majority of the boundary layer, which has thickness $O(R_1^{-\frac{1}{2}})$. This occurs when $|T - T_0| = O(R_1^{-\frac{1}{2}})$, that is, when

$$t - R_1^{\frac{1}{2}} t_s - R_1^{-\frac{1}{2}} T_0 = O(R_1^{-\frac{1}{2}}) \quad (4.5)$$

and

$$x - x_c - R_1^{\frac{1}{2}} x_s - R_1^{-\frac{1}{2}} X_0 = O(R_1^{-\frac{1}{2}}).$$

These are the Eulerian scalings, where the local streamwise and normal coordinates are of the same order, and the resulting inviscid problem is subject to the existence of a viscous sublayer of thickness $O(R_1^{-\frac{1}{2}})$. In other words, in the new stage defined by (4.5) the velocity and pressure disturbances become increased to $O(1)$ and so the Euler equations come into operation across the entire boundary layer. The eddy starts to span the boundary layer and the determination of its evolution then becomes a rather difficult vortex-sheet problem, which has still to be tackled.

5. Remarks

We should remark first that there are numerous other aspects in the overall flow field, similar to those discussed by Smith & Elliott (1985). These include different kinds of instability, namely the viscous-inviscid Tollmien-Schlichting kind, the inviscid short-scale Rayleigh kind, and the inviscid Kelvin-Helmholtz kind, although they need not be the most important instability processes in practice. Also, the theories for these other instabilities have yet to reach a sufficiently advanced stage to accommodate nonlinearities of the kind given by the present theory although, for example, a start has been made by Burggraf & Smith (1985) and by the present authors, and there are many computational studies in the literature. Again, the present theory addresses marginal separation only, as opposed to the more common triple-deck breakaway or localized separation. Nevertheless, since the observed separation occurs near the leading edge, the process of dynamic stall appears in many ways to be more closely connected with marginal separation than with general mid-chord separation, in its beginnings.

Beyond those beginnings, i.e. beyond the finite-time singularity proposed in the present work, yet faster timescales and increasingly shorter streamwise lengthscales come into operation and the local flow develops rapidly towards a nonlinear Euler stage, with the length- and the timescales shortening then to the scale of the boundary-layer thickness $O(R_1^{-\frac{1}{2}})$. Outside these fast local developments the flow can remain quasi-steady, or less unsteady, until other local breakdowns occur elsewhere. Locally, the final nonlinear Euler stage (§4) appears to be predominantly inviscid in nature, although it is certainly influenced by bursts of vorticity (Van Dommelen 1981; Elliott *et al.* 1983; Burggraf & Smith 1985) from the viscous sublayer at the solid surface. The degree of this extra bursting influence and the properties of the whole Euler stage need to be researched much further. Meanwhile, it is of some encouragement that the theory so far appears to agree qualitatively with the experimental findings on dynamic stall, in the sense that it shows how an initially slender embedded eddy (or eddies) of lengthscale much greater than the boundary-layer thickness can change dynamically, by means of bursting through the present interactive mechanism, into a thick blunt eddy spanning the whole boundary layer in the Euler stage. Beyond that stage, shedding of the eddy seems a distinct possibility.

The referees' and the editor's comments are gratefully acknowledged, and J. W. E. thanks the SERC for financial support during part of this research.

Appendix. Concerning the deviation of (3.7a)

Let us consider the general Whittaker equation for $H_\nu(k; \xi)$

$$\frac{d^2 H_\nu}{d\xi^2} + \left[-\frac{1}{4} + \frac{k}{\xi} + \frac{(\frac{1}{4} - \nu^2)}{\xi^2} \right] H_\nu = 0.$$

This has standard solutions $W_\nu(k; \xi)$, and $M_\nu(k; \xi)$ (Abramowitz & Stegun 1965). In the following section the asymptotic behaviour, as $k \rightarrow \infty$, of the above standard solutions is investigated and it is easily seen that their behaviour splits in two: an outer 'inviscid' solution when $\xi = O(|k|)$ and an inner 'viscous' zone when $\xi = O(|k|^{-1})$. In fact only the behaviour for k real and negative is discussed below. This involves modified Bessel functions in the inner region and exponential growth and decay in the outer region, although this can easily be extended to the case $\text{Re}(k) \leq 0$. The case for k real and positive and its extension to $\text{Re}(k) > 0$ can be discussed similarly although it is more complicated. In the inner region it involves the standard Bessel functions, while we must split the outer region into two with a 'critical layer' at $\xi = 4k$ requiring Airy functions to smooth the switch from oscillatory to exponential behaviour.

For $k < 0$ we see that as $|k| \rightarrow \infty$ the inner 'viscous' forms for the standard solutions are given by

$$\left. \begin{aligned} W_{\frac{3}{4}}(k; \xi) &\sim \frac{|k|^{\frac{1}{2}}}{\Gamma(\frac{5}{4} - k)} u \left\{ K_{\frac{3}{4}}(u) + O\left(\frac{1}{|k|^2}\right) \right\}, \\ M_{\frac{3}{4}}(k; \xi) &\sim \frac{3\pi^{\frac{1}{2}}}{8} \frac{1}{|k|^{\frac{3}{4}}} u \left\{ I_{\frac{3}{4}}(u) + O\left(\frac{1}{|k|^2}\right) \right\}, \end{aligned} \right\} \quad (\text{A1})$$

where $\xi = |k|^{-1}(\frac{1}{2}u^2)$ and $I_{\frac{3}{4}}$, $K_{\frac{3}{4}}$ are modified Bessel functions (Abramowitz & Stegun 1965). From the properties of Bessel functions we know that in the double limit $|k| \rightarrow \infty$, $u \rightarrow \infty$ we have

$$\left. \begin{aligned} W_{\frac{3}{4}}(k; \xi) &\sim \frac{|k|^{\frac{1}{2}}}{\Gamma(\frac{5}{4} - k)} (\frac{1}{2}\pi)^{\frac{1}{2}} u^{\frac{1}{2}} \exp(-u), \\ M_{\frac{3}{4}}(k; \xi) &\sim \frac{1}{|k|^{\frac{3}{4}}} \frac{\Gamma(\frac{5}{2})}{2(2\pi)^{\frac{1}{2}}} u^{\frac{1}{2}} \exp(u). \end{aligned} \right\} \quad (\text{A2})$$

Hence the outer 'inviscid' forms for our standard solutions are given by

$$\begin{aligned} M_{\frac{3}{4}}(k; \xi) &\sim \frac{3}{8} \frac{1}{|k|^{\frac{3}{4}}} \left[\left(\frac{4\eta}{4 + \eta} \right)^{\frac{1}{4}} + \dots \right] \exp[|k|B(\eta)], \\ W_{\frac{3}{4}}(k; \xi) &\sim \frac{\pi^{\frac{1}{2}} |k|^{\frac{1}{2}}}{\Gamma(\frac{5}{4} - k)} \left[\left(\frac{4\eta}{4 + \eta} \right)^{\frac{1}{4}} + \dots \right] \exp[-|k|B(\eta)], \end{aligned}$$

where $\xi = |k|\eta$ and

$$B(\eta) = 2\{\log[(1 + \frac{1}{4}\eta)^{\frac{1}{2}} + \frac{1}{2}\eta^{\frac{1}{2}}] + \frac{1}{2}\eta^{\frac{1}{2}}(1 + \frac{1}{4}\eta)^{\frac{1}{2}}\}.$$

For $k < 0$ we recall that the left-hand side of (3.5a) is given by

$$[F(k) + (\frac{1}{2}\pi)^{\frac{1}{2}} |k| G(k)], \quad (\text{A3})$$

where instead of the representations given by (3.5*b, c*) we can write $F(k)$ and $G(k)$ as integrals of Whittaker functions,

$$F(k) = \sqrt{2\Gamma(\frac{5}{4}-k)} \int_0^\infty \frac{1}{\xi^{\frac{3}{4}}} W_{\frac{3}{4}}(k; \xi) d\xi,$$

$$G(k) = \frac{2\Gamma(\frac{5}{4}-k)}{\Gamma(\frac{5}{2})} \int_0^\infty \frac{1}{\xi^{\frac{3}{4}}} M_{\frac{3}{4}}(k; \xi) \left[\int_\xi^\infty \frac{1}{t^{\frac{3}{4}}} W_{\frac{3}{4}}(k; t) dt \right] d\xi.$$

From (A 1) and (A 2) we see that as $|k| \rightarrow \infty$ the contribution to $F(k)$ comes entirely from the inner solution, since $W_{\frac{3}{4}}(k; \xi)$ is exponentially small in the outer region. Therefore

$$F(k) \sim 4|k|^{\frac{1}{2}} \left\{ \int_0^\infty \frac{1}{u^{\frac{3}{2}}} K_{\frac{3}{2}}(u) du + O\left(\frac{1}{|k|^2}\right) \right\} = -4(\frac{1}{2}\pi)^{\frac{1}{2}} |k|^{\frac{1}{2}} \left\{ 1 + O\left(\frac{1}{|k|^2}\right) \right\}. \tag{A 4}$$

However for $G(k)$ we see that the product of exponential growth and decay of the standard solutions in the outer region leads to a contribution from that region that cannot be neglected. If we write $G(k) = G^{(1)}(k) + G^{(2)}(k)$ where $G^{(1)}$ is the inner contribution then we see that as $|k| \rightarrow \infty$

$$G^{(1)}(k) \sim \frac{8}{|k|^{\frac{1}{2}}} \left\{ \int_0^\infty \frac{1}{u^{\frac{3}{2}}} K_{\frac{3}{2}}(u) \left[\int_0^\infty \frac{1}{s^{\frac{3}{2}}} I_{\frac{3}{2}}(s) ds \right] du + O\left(\frac{1}{|k|^2}\right) \right\}$$

$$= \frac{8}{|k|^{\frac{1}{2}}} \left\{ \int_0^\infty \frac{1}{u} K_{\frac{3}{2}}(u) I_{\frac{3}{2}}(u) du + O\left(\frac{1}{|k|^2}\right) \right\}$$

$$= \frac{4}{|k|^{\frac{1}{2}}} \left\{ 1 + O\left(\frac{1}{|k|^2}\right) \right\}. \tag{A 5}$$

Similarly the outer contribution $G^{(2)}(k)$ has the form

$$G^{(2)}(k) \sim \frac{1}{|k|^{\frac{1}{2}}} \left\{ \int_0^\infty \frac{1}{\eta^{\frac{3}{2}}} \left(\frac{4\eta}{4+\eta}\right)^{\frac{1}{2}} \exp(|k|B(\eta)) \left[\int_\eta^\infty \frac{1}{s^{\frac{3}{2}}} \left(\frac{4s}{4+s}\right)^{\frac{1}{2}} \exp(-|k|B(s)) ds \right] d\eta \right\}$$

$$\sim \frac{1}{|k|^{\frac{1}{2}}} \left\{ \int_0^\infty \frac{1}{\eta^{\frac{3}{2}}} \left(\frac{4\eta}{4+\eta}\right) d\eta + O\left(\frac{1}{|k|^2}\right) \right\}$$

$$= -\frac{1}{|k|^{\frac{1}{2}}} (\frac{1}{2}\pi) \left\{ 1 + O\left(\frac{1}{|k|^2}\right) \right\}. \tag{A 6}$$

From (A 4) and (A 5) we see that the larger ‘viscous’ contributions to (A 3) cancel, to the leading order, and so the leading-order term is a purely ‘inviscid’ one. Hence we see that as $k \rightarrow -\infty$

$$F(k) + (\frac{1}{2}\pi)^{\frac{1}{2}} |k| G(k) = -(\frac{1}{2}\pi)^{\frac{1}{2}} \frac{1}{|k|^{\frac{1}{2}}} \left\{ 1 + O\left(\frac{1}{|k|^2}\right) \right\}. \tag{A 7}$$

Therefore we see that, to leading order, (A 3) is given by (A 7) and so we can replace equation (3.5*a*) by (3.7*a*) for $(-k) \gg 1$.

REFERENCES

ABRAMOWITZ, M. & STEGUN, I. A. 1965 *Handbook of Mathematical Functions*. Dover.
 BURGGRAB, O. R. & SMITH, F. T. 1985 On the development of large-sized short-scaled disturbances in boundary layers. *Proc. R. Soc. Lond.* A **399**, 25–55.
 DUCK, P. W. 1985 Laminar flow over unsteady humps: the formation of waves. *J. Fluid Mech.* **160**, 465–498.

- ELLIOTT, J. W., COWLEY, S. J. & SMITH, F. T. 1983 Breakdown of boundary layers, (i) on moving surfaces, (ii) in semi-similar unsteady flow, (iii) in fully unsteady flow. *Geophys. Astrophys. Fluid Dyn.* **25**, 77–138.
- GOLDSTEIN, S. 1948 On laminar boundary-layer flow near a position of separation. *Q. J. Mech. Appl. Maths* **1**, 43–69.
- MCCALLISTER, K. W. & CARR, I. W. 1979 *Trans. ASME I: J. Fluids Engng* **10**, 376.
- MCCROSKEY, W. J. 1982 Unsteady airfoils. *Ann. Rev. Fluid Mech.* **14**, 285–311.
- MOORE, D. W. 1979 The spontaneous appearance of a singularity in the shape of an evolving vortex sheet. *Proc. R. Soc. Lond. A* **365**, 105–119.
- RYZHOV, O. S. & SMITH, F. T. 1984 Short-length instabilities, breakdown and initial-value problems in dynamic stall. *Mathematika*. **31**, 163.
- SMITH, F. T. 1979 On the non-parallel flow stability of the Blasius boundary layer. *Proc. R. Soc. Lond. A* **360**, 91–109.
- SMITH, F. T. 1982 Concerning dynamic stall. *Aero Q.* November, 331–352.
- SMITH, F. T. & ELLIOTT, J. W. 1985 On the abrupt turbulent reattachment downstream of leading-edge laminar separation. *Proc. R. Soc. Lond. A* **401**, 1–27.
- SMITH, F. T. & MERKIN, J. H. 1984 Triple-deck solutions for subsonic flow past humps, steps, concave or convex corners and wedged trailing edges. *J. Comput. Fluids* **10**, 7–25.
- STEWARTSON, K. 1970 Is the singularity at separation removable? *J. Fluid Mech.* **44**, 347–364.
- STEWARTSON, K., SMITH, F. T. & KAUPS, K. 1982 Marginal separation. *Stud. Appl. Maths* **67**, 45–61.
- TELIONIS, D. P. 1981 *Unsteady Viscous Flows*. Springer.
- VAN DOMMELEN, L. L. 1981 Unsteady boundary layer separation. Ph.D. thesis, Cornell University.